ABSENCE OF TECTONIC ROTATIONS IN MIOCENE-PLIOCENE MARINE SEDIMENTS FROM MEJILLONES PENINSULA AND BAHIA INGLESA, NORTHERN CHILE

Claudio A Tapia[1]*, Gary S. Wilson[2] & Scott E. Ishman[3]

[1] Departamento de Obras Civiles y Geología, Universidad Católica de Temuco, Temuco, Chile
[2] Department of Marine Science, University of Otago, Dunedin, New Zealand
[3] Department of Geology, Southern IL University, Carbondale, IL, USA
*e-mail: Claudio.tapia@uct.cl

ABSTRACT

We present paleomagnetic data of a total of nine marine sedimentary sections, two of them spanning early Miocene to mid Pliocene age at Mejillones Peninsula, and seven sections covering mid Miocene to early Pliocene age at Bahia Inglesa. Results shows no tectonic rotation at both localities confirming that deformation is not important at the Central Andes since 20 Ma, as is propoesed by Arriagada *et al*. (2008). Data also agrees with the deformation conceptual model related with the migration and subduction of the Juan Fernandez Ridge presented in Arriagada *et al*. (2013) and with the proposed bending of the Juan Fernandez Ridge mechanism of Le Roux *et al*. (2016), which consequently caused a less intense but broader stress field that could have prevented a mayor deformation of the margin, similar to the Maipo Orocline (Arriagada *et al*., 2013).

Keywords: Miocene, Pliocene, Juan Fernandez, Rotation, Paleomagnetic.

RESUMEN

Presentamos datos paleomagnéticos de un total de nueve secciones sedimentarias marinas, dos de ellas que abarcan desde el Mioceno Inferior al Plioceno Medio en la Península de Mejillones, y siete secciones que cubren el Mioceno Medio hasta el Plioceno Inferior en Bahía Inglesa. Los resultados muestran rotaciones tectónicas nulas en ambas localidades confirmando que la deformación no es importante en los Andes Centrales desde 20 Ma, como ha sido propuesto por Arriagada *et al*. (2008). Los datos también corroboran el modelo conceptual de deformación relacionado con la migración y la subducción de la Dorsal Juan Fernández presentada en Arriagada *et al*. (2013) y con la propuesta de flexión de la Dorsal Juan Fernández de Le Roux *et al*. (2016), lo que consecuentemente causó un campo de estrés menos intenso, pero más amplio que podría haber evitado una deformación mayor del margen, similar al Oroclinal del Maipo (Arriagada *et al*., 2013).

Palabras Claves: Mioceno, Plioceno, Juan Fernandez, Rotación, Paleomagnético.

1. Introduction

In the central Andes three remarkable tectonic features have been recognized: 1) The Abancay Deflection; 2) The Arica-Bolivian Orocline; and 3) The Altiplano high mesa; The genesis and relation between them have been extensively studied over the past 30 years in studies involving geodetic data (Allmendinger *et al*., 2005); seismic data (Oncken *et al*., 2006); and structural data (Baby *et al*., 1997; Kley, 1999; McQuarrie, 2002). A restoration of central Andean deformation was proposed by Arriagada *et al*. (2008), using data of magnitude and age of tectonic block rotations and estimation of shortening from balanced cross sections.

The paleomagnetic data used to restore tectonic block rotations were compiled from Roperch *et al*. (2006) for the northern central Andes and from Arriagada *et al*. (2006) for the southern central Andes. However, only one site at Playa Chorrillos locality on sediments from the Bahia Inglesa Formation was available for Neogene forearc rocks at the south-central Andes. In both studies, it was suggested that no rotations have occurred among the forearc for rocks younger than 20 Ma.

On the other hand, Le Roux *et al*. (2016), based on stratigraphic environment interpretation and general correlations of sections from Bahia Inglesa together with $^{87}Sr/^{86}Sr$ dating suggested an orocline formation of the Juan Fernandez Ridge due to friction with the overlying continental plate, similar to what has been observed around the Nazca Ridge in Peru to explain a less intense southward uplift–subsidence–uplift tectonic sequence controlled by a broader but less intense associated stress field. However, Arriagada *et al*. (2013) reported the Maipo Orocline feature between ~33º and 36º S and related its origin to a coupled Bolivian Orocline rotational component amplified later by the Juan Fernaandez Ridge subduction.

The data presented here contributes to constrain of the style and timing of the Miocene to Recent geodynamic evolution in the central Chilean Andes.

2. Geological setting

The two main locations studied here are located in the Coastal Platform, which is bounded to the east by the Coastal Cordillera. The Coastal Cordillera is a continuous north-south elongated physiographic unit present between 22ºS and 28ºS latitude, and has an average elevation about 1500 m a.s.l., and a maximal elevation of 2700 m a.s.l. The Coastal Platform is only preserved at discrete locations along the coast of northern Chile: At 23ºS latitude, as the Mejillones Peninsula itself (Figure 1B); and between Caldera and the Copiapo River mouth (Figure 1C), as a 10 km wide, slightly tilted to the west, emergent platform.

At the Peninsula of Mejillones and Caldera Area latitudes, the Coastal Cordillera, and the local Coastal Platform plus the Continental slope shows extensional tectonic modification since at least Miocene times and has been interpreted to be the result of tectonic erosion under the South American plate that produced continental collapse toward the trench (Hartley and Jolley, 1995; Niemeyer *et al*., 1996; Delouis *et al*., 1996; Hartley et al., 2000). The local extension pattern has been correlated to a major regional system of the outer fore arc recognized to the north of the Mejillones Peninsula (González et al., 2003). At both locations, extensional patterns have developed as an E-W trending system (Marquardt et al., 2004; Victor et al., 2011). At Caldera, an uppermost Pliocene NW-SE to E-W compression is evident (Marquardt et al., 2004) and since middle Pleistocene times a NW-SE extension has been active and moderate to high vertical uplift rate is observed from marine abrasion terraces (Marquardt et al., 2004; Quezada et al., 2010).

At the two main localities, the oldest rocks comprise Paleozoic Metamorphic rocks intruded by Jurassic plutons (Figure 1B). At Mejillones Peninsula, Cretaceous marine and continental sedimentary rocks overlie sequences of Jurassic volcanic rocks (Figure 1C). Nonconformably overlying the Paleozoic-Mesozoic basement is a predominately marine, continental slope to littoral sequence, mostly late Neogene (La Portada Formation at Mejillones Peninsula and Bahia Inglesa Formation at Caldera, sampled in this work) to Quaternary in age, that interlace with contemporaneous continental, alluvial, eolian, and fluvial sediments.

2. Sampling and methods

Standard discrete cylindrical paleomagnetic samples were collected using a portable gasoline-powered drill system. Individual samples were oriented using a magnetic compass, with occasional cross checking from solar orientation.

At Mejillones, two main sections were sampled (Figure 1B), one at the ‘‘Caleta Herradura’’ Bay (coast of the central part of the Mejillones Peninsula) and other, the Tiburon Basin, located in the central part of the peninsula. The outcrop of the Caleta Herradura succession exposes a vertical face of 50–100 m high and is 2 km in length. Thirty-one sites were obtained from a 380 m thick stratigraphic succession. At the Tiburon Basin, the studied section is a composite from base to top (Figure 1B, Tapia *et al*., 2015)

At Caldera 83 sample sites were distributed over six localities (Figure 1C): Quebrada Blanca (8 sites), Rocas Negras (11 sites), Quebrada Angosta (10 sites), High Section (3 sites), Quebrada Playa Chorrillos (11 sites), and Quebrada La Higuera (41 sites).

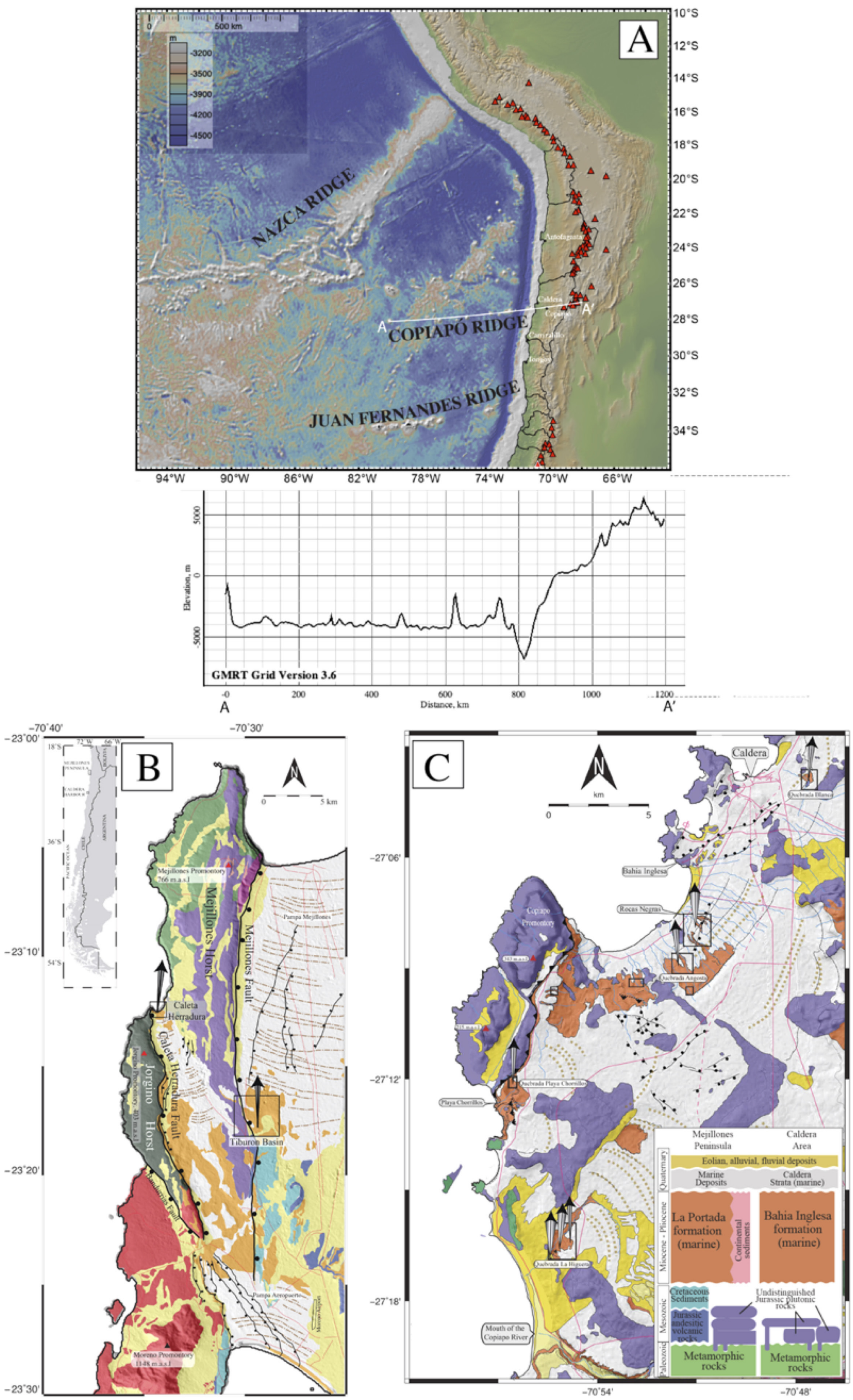

Figure 1. A. Color relief map of Central Andes produced with GeoMapApp. Red triangles are actual active volcanos form the Smithsonian Institution, Global Volcanism Program. A-A'Profile is indicated with a white line

on map. **B**. Geologic map of Mejillones Peninsula, modified from Cortés *et al*. (2007). **C**. Simplified geologic map of Caldera Area modified from Godoy *et al*. (2003). Arrows and wedges are calculated rotation and associated error for both localities. Map colors are as in stratigraphic scheme. Rectangles indicate sampling locations.

Samples were measured on 2G Enterprises cryogenic magnetometers at the Paleomagnetism Laboratory of Oxford University and the Otago Paleomagnetic Research Facility at the University of Otago. At the Otago Paleomagnetic Research Facility, isothermal remanent magnetization (IRM) was imparted on selected samples with an ASC scientific impulse magnetizer and then measured with a Molspin Spinner magnetometer. Thermomagnetic susceptibility was determined with a MFK1-A AGICO susceptibilimeter with a CS-3 attached furnace for high temperature measurements in an Argon atmosphere to minimize oxidation of iron-rich clays. Magnetic hysteresis loops were measured with a Princeton Micromag 2900 AGM Magnetometer at the Instituto Nazionale di Geofisica e Vulcanologia Paleomagnetic Laboratory, Rome.

Steps of all measurements performed here were the standard for paleomagnetic and rock magnetic studies and are well detailed in Tapia & Wilson, (2014); and in Tapia *et al*., (2015).

3. Rock magnetism and paleomagnetic behaviour

Remanent magnetizations generally comprises three components (Figure 2): a low blocking temperature (Tb) component, below 150º C, close to the present-day field in direction, interpreted as a thermoviscous component; an intermediate Tb component, between 150º C and 290º C, overprinted by the low and the high Tb components, considered as the survival of the characteristic detrital magnetization; and a high Tb component, above 290º C, thought to be of diagenetic origin. Detrital magnetite, titanomagnetite, and low titanium maghemite are identified as the main carrier of the magnetic remanence (Figure 2). Rock magnetic results of a minor group of samples at both locations detected the presence of a high-coercivity mineral, possibly hematite, interpreted to carry the high Tb component and to represent oxidation of minerals in postdepositional processes (Figure 2).

4. Variation of flattening on paleomagnetic results

Flattening calculations for sites are summarized in Table 1. Most of the paleomagnetic mean directions calculated had low flattening (below 5), less inclined than expected for sediments (King, 1955; Tauxe *et al*., 2008).

Data from Tiburon Basin show up to 6.3º± 3.7 of flattening. Direction flattening within the Tiburon Basin may be related to the facies composition of the section. The lower part of Tiburon Basin section, where most of the samples were taken, has a high content of diatoms resulting in lower density sediments at deposition times, subjected to an increased degree of post depositional compaction.

At Caldera, the Rocas Negras section showed 3.5º of flattening, however, the error is higher than the degree of flattening (± 6.6º). This result may be related to the low number of samples and the low quality of the signal. At the Quebrada La Higuera location, section 4 showed flattening as much as 10.7º and a high error as well (± 7º). At the outcrop, this section showed a differential inclination of the strata (increasing inclination from bottom to top) due to tectonic folding. Therefore, it is assumed that strata were exposed to compression that could have introduced the higher degree of flattening observed.

5. Absence of tectonic rotations

Rotation are calculated and summarized in Table 1 and shown in Figure 1 and 3. At Mejillones Peninsula, little (5.5º± 3.7) clockwise rotation was identified for mid to upper Miocene marine sediments of Caleta Herradura, however, no pattern within the section could confirm this, and it may be related to local folding

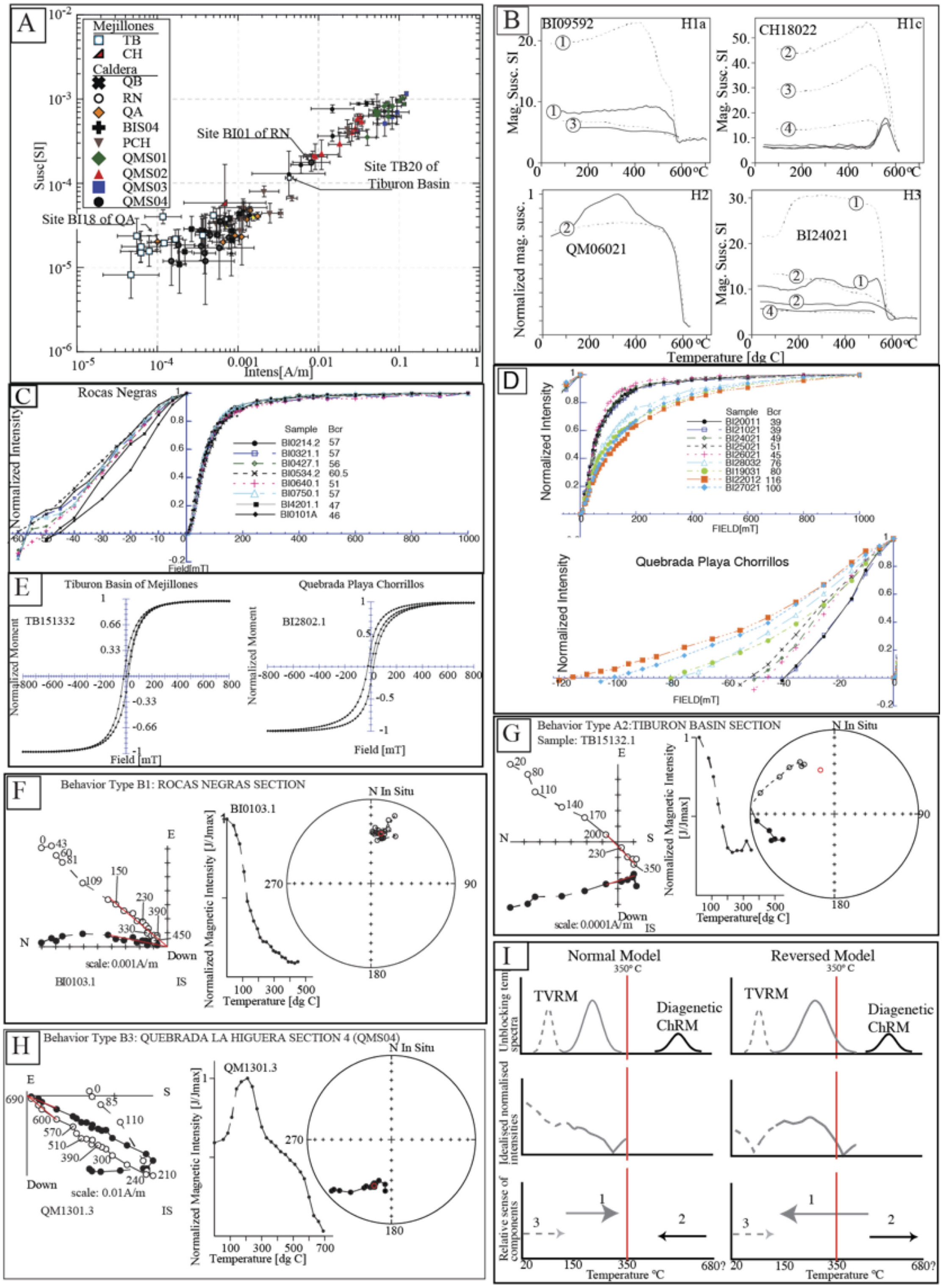

Figure 2. **A**. Geometric mean of NRM versus magnetic susceptibility. **B**. Selected thermo-susceptibility step heated curves (1) above 700º C; (2) above 600º C; (3) just below 600º C and (4) just above 500º C. **C–D**. IRM curves. Bcr is coercivity of remanence. **E**. Hysteresis Loops from selected samples of Mejillones and Caldera. **F–H**. Selected vector component, stereographic, and stepwise intensity plots. **I**. Multicomponent model. Top is blocking temperature spectrum. Central is typical intensity demagnetisation curve. Bottom is the relative polarity sense of the components. Further explanation in: Tapia, Wilson, 2014; Tapia *et al*., 2015.

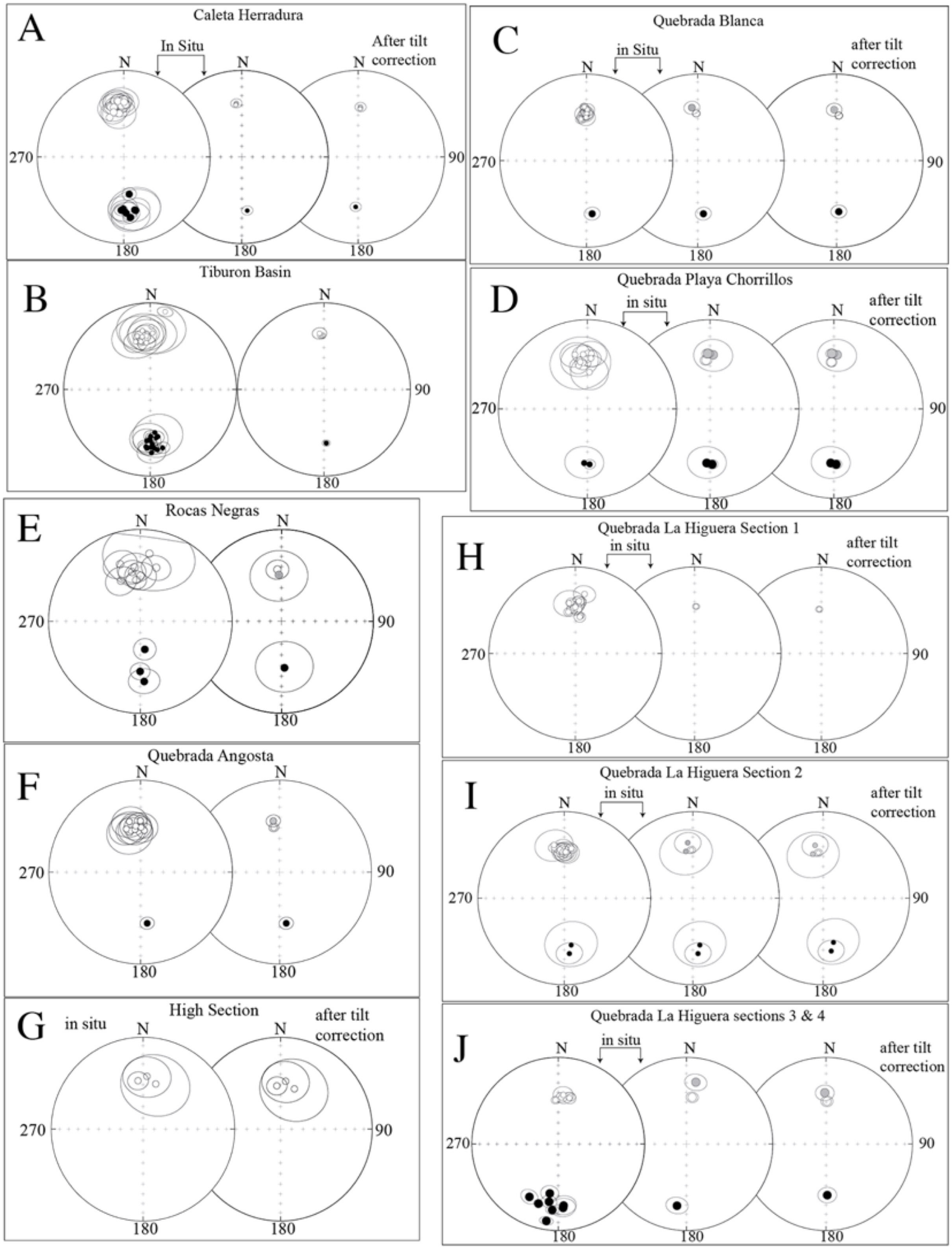

Figure 3. Paleomagnetic characteristics directions of both studied localities. Equal area stereographic plots (left plot are all sites, center and right are mean directions). Open (solid) circles displaying normal (reversed) directions. Ellipses correspond to 95% semi angle of confidence. Reversed mean direction plotted in upper north hemisphere distinguished with grey.

Table 1. Locality rotation and flattening calculation from expected paleomagnetic direction

Locality	Age Ma	Latitude [°]	Longitude [°]	N	Observed Dec [°]	Observed Inc [°]	Observed α95 [°]	Expected Dec [°]	Expected Inc [°]	Rotation R [°]	Rotation ±∂R [°]	Flattening F [°]	Flattening ±∂F [°]
Mejillones													
Tiburon Basin	5	-23.304	-70.490	28	356.6	-36.8	3.1	356.7	-43.1	-0.1	3.9	-6.3	3.7
Caleta Herradura	15	-23.210	-70.572	31	2.6	-42.9	2.1	357.1	-47.0	5.5	3.7	-4.1	3.5
Caldera													
Quebrada Blanca	5	-27.065	-70.793	8	2.2	-46.0	3.4	356.6	-47.8	5.6	4.6	-1.8	3.7
Rocas Negras	5	-27.133	-70.850	11	355.6	-44.3	7.6	356.6	-47.8	-1.0	8.8	-3.5	6.6
Quebrada Angosta	5	-27.148	-70.857	10	352.5	-48.8	3.8	356.6	-47.9	-4.1	5.2	0.9	3.9
Quebrada Playa Chorrillos	5	-27.240	-70.94	11	357.8	-44.9	4.1	356.6	-48.0	1.2	5.2	-3.1	4.1
Quebrada La Higuera Section 1&2	5	-27.274	-70.915	28	355.6	-46.8	2.3	356.6	-48.0	-1.0	3.6	-1.2	3.1
Quebrada La Higuera Section 3	10	-27.276	-70.915	5	1.2	-49.1	5.3	357.3	-50.4	3.9	7.1	-1.3	5.1
Quebrada La Higuera Section 4	15	-27.278	-70.918	8	358.6	-40.5	8.0	357.2	-51.2	1.4	9.0	-10.7	7.0

not accommodated by the broad bedding correction applied to the paleomagnetic samples. The Pliocene Tiburon Basin section did not show rotation. Caldera sections, Quebrada Blanca and section 3 of Quebrada La Higuera, show little clockwise rotation. At Quebrada Blanca the error is as large as the rotation and Quebrada La Higuera sections below and above section 3 do not show any rotation at all.

6. Discussion and conclusions

The results obtained here confirms the preliminary results from Arriagada *et al*. (2008) that suggested deformation is important at the Central Andes prior 20 Ma. Data is in good agreement with the conceptual models of deformation of the margin due to de subduction evolution of the Juan Fernandez Ridge presented by Arriagada *et. al*. (2013) and Le Roux *et al*. (2016).

7. Acknowledgements

This research was funded by the Foundation for Research Science and Technology of New Zealand (grant reference numbers: UOOX0207 & UOOX0712), U.S. National Science Foundation (grant reference numbers: 0119298 & 0203555) and CONICYT – Chile (PhD scholarship to the first author, Project Id.: 05-DOCBIRF-41).

8. References

Allmendinger, R. W., Smalley, R., Bevis, M., Caprio, H., and Brooks, B. (2005). Bending the Bolivian orocline in real time. *Geology 33* (11), 905– 908.

Arriagada, C., Ferrando, R., Córdova, L., Morata, D. & Roperch, P. 2013. The Maipo Orocline: A first scale structural feature in the Miocene to Recent geodynamic evolution in the central Chilean Andes. *Andean Geology 40* (3), 419–437.

Arriagada, C., Roperch, P., Mpodozis, C., and Cobbold, P. R. (2008). Paleogene building of the Bolivian Orocline: Tectonic restoration of the central Andes in 2-D map view. *Tectonics 27*, 14 pp.

Arriagada, C., Roperch, P., Mpodozis, C., and Fernandez, R. (2006). Paleomagnetism and tectonics of the southern Atacama Desert (25-28ºS). *Tectonics 25* (TC4001), 1–26.

Baby, P., Rochat, P., Mascle, G. and Hérail, G. (1997). Neogene shortening contribution to crustal thickening in the back arc of the Central Andes. *Geology 25* (10):883–886.

Cortés, J., Marquardt, C., González, G., Wilke, H. & Marinovic, N. 2007. Cartas Mejillones y Península de Mejillones, Región de Antofagasta, Escala 1:100000. *SERNAGEOMIN, Carta Geológica de Chile, Serie Geología Básica* (n.103-104) (Santiago), 58 pp.

Delouis, B., Cisternas, A., Dorbath, L., Rivera, L. & Kausel, E. 1996. The Andean subduction zone between 22 and 25ºS (northern Chile): precise geometry and state of stress. *Tectonophysics 259* (1–3), 81–100.

Godoy, E., Marquardt, C. & Blanco, N. 2003. Carta Caldera, Región de Atacama. *SERNAGEOMIN, Carta Geológica de Chile, Serie Geología Básica* mapa escala 1:100.000 (76), 38 pp.

González, G., Cembrano, J., Carrizo, D., Macci, A. & Schneider, H. 2003. The link between forearc tectonics and Pliocene-Quaternary deformation of the Coastal Cordillera, northern Chile. *Journal of South American Earth Sciences 16* (5), 321–342.

Hartley, A.J. & Jolley, E.J. 1995. Tectonic implications of late Cenozoic sedimentation from the Coastal Cordillera of northern Chile (22-24ºS). *Journal of the Geological Society 152* (1), 51–63.

Hartley, A.J., May, G., Chong, G., Turner, P., Kape, S.J. & Jolley, E.J. 2000. Development of a continental forearc: A Cenozoic example from the Central Andes, northern Chile. *Geology 28* (4), 331–334.

King, R. F. (1955). The Remanent Magnetism of Artificially Deposited Sediments. *Geophysical Journal International 7* (s3), 115–134.

Kley, J. (1999). Geologic and geometric constraints on a kinematic model of the Bolivian orocline. *Journal of South American Earth Sciences 12* (2), 221–235.

Le Roux, J.P., Achurra, L., Henríquez, Á., Carreño, C., Rivera, H., Suárez, M.E., Ishman, S.E., Pyenson, N.D. & Gutstein, C.S. 2016. Oroclinal bending of the Juan Fernández Ridge suggested by geohistory analysis of the Bahía Inglesa Formation, north-central Chile. *Sedimentary Geology 333*, 32–49.

Marquardt, C., Lavenu, A., Ortlieb, L., Godoy, E. & Comte, D. 2004. Coastal neotectonics in Southern Central Andes: uplift and deformation of marine terraces in Northern Chile (27º S). *Tectonophysics 394* (3–4), 193–219.

McQuarrie, N. (2002). Initial plate geometry, shortening variations, and evolution of the Bolivian orocline. *Geology 30* (10):867–870.

Niemeyer, H., González, G. & Martínez-De Los Ríos, E. 1996. Evolución tectónica cenozoica del margen continental activo de Antofagasta, norte de Chile. *Revista Geológica de Chile 23*, 165–186.

Oncken, O., Hindle, D., Kley, J., Elger, K., Victor, P., and Schemmann, K. (2006). Deformation of the Central Andean Upper Plate System - Facts, Fiction, and Constraints for Plateau Models. Frontiers in Earth Sciences. Springer Berlin Heidelberg. 10.1007/978-3-540-48684-81.

Quezada, J., Cerda, J.L. & Jensen, A. 2010. Efectos de la tectónica y el clima en la configuración morfológica del relieve costero del norte de Chile. *Andean geology 37*, 78-109.

Roperch, P., Sempere, T., Macedo, O., Arriagada, C., Fornari, M., Tapia, C., García, M., and Laj, C. (2006). Counterclockwise rotation of late Eocene-Oligocene fore-arc deposits in southern Peru and its significance for oroclinal bending in the central Andes. *Tectonics 25* (TC3010).

Tapia, C.A. & Wilson, G.S. 2014. Rock magnetic properties and paleomagnetic behavior of Neogene marine sediments from northern Chile. *Geochem. Geophys. Geosyst 15* (11), 4400–4423.

Tapia, C.A., Wilson, G.S., Ishman, S.E., Wilke, H.G., Wartho, J.-A., Winter, D. & Martinez-Pardo, R. 2015. An integrated sequence stratigraphic and chronostratigraphic analysis of the Pliocene, Tiburon Basin succession, Mejillones Peninsula, Chile. *Global and Planetary Change 131* (0), 124–147.

Tauxe, L. 1998. *Paleomagnetic Principles and Practice*, Kluwer Academic Publishers, The Netherlands, 312 pp.

Tauxe, L., Kodama, K.P. & Kent, D.V. 2008. Testing corrections for paleomagnetic inclination error in sedimentary rocks: A comparative approach. *Physics of the Earth and Planetary Interiors 169* (1–4), 152–165.

Victor, P., Sobiesiak, M., Glodny, J., Nielsen, S. N., and Oncken, O. (2011). Long-term persistence of subduction earthquake segment boundaries: Evidence from Mejillones Peninsula, northern Chile. J. Geophys. Res. *116* (B2), B02402.